Waveguide-saturable absorber fabricated by femtosecond pulses in YAG:Cr^{4+} crystal for *Q*-switched operation of Yb-fiber laser

Andrey G. Okhrimchuk,[1,3,*] Vladimir K. Mezentsev,[1] Vladislav V. Dvoyrin,[3] Andrey S. Kurkov,[4]
Evgeny M. Sholokhov,[4] Sergey K. Turitsyn,[1] Alexander V. Shestakov,[2] and Ian Bennion[1]

[1]*Photonics Research Group, Aston University, Birmingham, B4 7ET, UK*
[2]*Elements of Laser Systems Co., 3 Vvedensky Street, Moscow 117342, Russia*
[3]*Fiber Optics Research Center RAS, 38 Vavilov Street, Moscow 119333, Russia*
[4]*General Physics Institute RAS, 38 Vavilov Street, Moscow 119333, Russia*
*Corresponding author: a.okhrimchuk@aston.ac.uk

A waveguide-saturable absorber with low propagation loss is fabricated by femtosecond pulses in YAG:Cr^{4+} crystal. *Q*-switch operation of a Yb fiber laser with the new saturable absorber having absorption saturation parameters similar to the bulk YAG:Cr^{4+} crystal is demonstrated. © 2009 Optical Society of America

OCIS codes: 220.4000, 140.3540.

Q-switched fiber lasers operating at 1 μm have found many important applications in material processing. Passive *Q* switching in fiber lasers is especially attractive because of its high efficiency and configuration simplicity. The key element of a passively *Q*-switched laser is a saturable absorber that can be implemented in a variety of ways, e.g., using nonlinear polarization evolution, doped fiber, semiconductor saturable absorber mirror, and others. An all-fiber or waveguide architecture of a *Q*-switch modulator is of particular interest because of its reliability and the associated simplicity of laser design. However, the number of available materials that can be successfully employed as a saturable absorber, especially for high-energy applications, is limited. For instance, a straightforward solution based on a silica fiber doped with ions possessing saturable transitions [1,2] has restrictions given by spectroscopic properties of the transition metal or rare-earth ions in the silica matrix. In the meantime, the YAG:Cr^{4+} crystal is the most popular saturable absorber material for solid-state lasers owing to its high absorption cross section and the low excited-state lifetime of the fourfold coordinated Cr^{4+} ion in the YAG crystal, together with the high damage threshold and good thermal conductivity of the latter. In this Letter we address the problem of smooth integration of a widely available bulk saturable absorber in a fiber laser by means of fabrication of a waveguide compatible with the fiber. Recent progress in femtosecond waveguide inscription in YAG crystals [3–5] paves the way to fabrication of a waveguide-saturable absorber (WSA) in a YAG:Cr^{4+} crystal. A waveguide-based design for a saturable absorber built upon the YAG:Cr^{4+} crystal has been recently reported [6,7]. In this Letter we present the novel WSA incorporated in a Yb fiber laser by direct butt-coupling to a conventional active fiber. *Q*-switched operation of a fiber laser integrated with the waveguide YAG:Cr^{4+} saturable absorber is demonstrated.

A waveguide was fabricated with a depressed cladding in a YAG:Mg^{2+},Cr^{4+} crystal under the crystal surface at 150 μm depth. The concentration of the fourfold coordinated Cr^{4+} was 0.72×10^{-18} cm^{-3}. The experimental setup for waveguide inscription was similar to that described in [3,8]. A femtosecond laser beam from a Ti-sapphire laser system operating at 800 nm at a 1 kHz repetition rate (Spitfire, Spectra Physics) was used for waveguide microfabrication. The laser produces pulses with a 115 fs pulse width. A 2 mm × 5 mm × 20 mm crystal sample was placed on a high-precision 3-D Aerotech translation stage. The laser beam was focused under the crystal surface with a Mitutoyo lens (NA = 0.55). The crystal was translated at a constant speed of 0.5 mm/s to inscribe smooth tracks with a lowered refractive index.

In this work we have utilized a femtosecond laser beam with an elliptic cross section. It proves to produce much more homogeneous tracks in YAG crystals compared to a standard beam of circular cross section [8]. Such an approach leads to dramatic reduction of scattering loss. To achieve this, a plane-concave cylindrical lens with a focal distance of 34 cm was used before the Mitutoyo lens to produce a waist of elliptical cross section. Normally, the two elliptical waists with mutually orthogonal orientations of principal axes were formed by the cylindrical lens. Typically, more than a half of the input pulse energy was absorbed in the first waist nearest to Mitutoyo lens [8]. Therefore, for the moderate input energies used in our experiments, the inscription threshold was not reached in the second waist. Thus, tracks were inscribed by the first waist with a principal axis parallel to the track.

The crystal was cut perpendicular to the waveguide direction in order to obtain waveguides of different lengths appropriate for waveguide characterization and applications in a *Q*-switched fiber laser. The crystal edges were polished. A microscopic image of the waveguide end is shown in Fig. 1. An elementary structural unit (a single track) is produced by straight translation of the crystal with constant velocity so that a femtosecond beam waist crosses the crystal from one edge to another. The cross section of
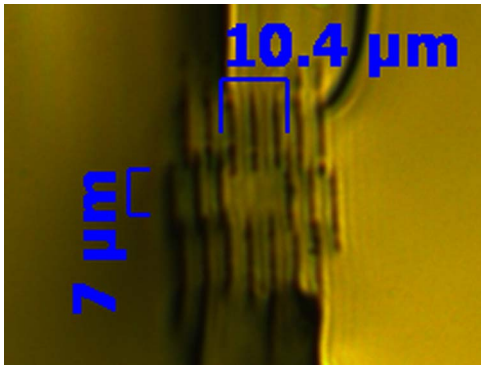
Fig. 1. (Color online) Microscope picture of the depressed cladding waveguide end.

the track has an oval shape with an aspect ratio in excess of 10. The refractive index inside those tracks is lowered by 3×10^{-3} compared to the unperturbed value in the bulk of the crystal. As a result, the array of tracks forms a waveguide cladding, while a core is formed by a nonperturbed region of the crystal. We wish to emphasize that the waveguide is formed due to the lowered refractive index in the cladding (depressed cladding) as an alternative to the design proposed in [5].

Numerical mode analysis of the developed waveguide structure was performed with a commercial code [9]. The electromagnetic eigenvalue problem was solved by the finite-element method. It was found that the structure maintains two fundamental modes with orthogonal polarizations with very similar, almost radially symmetric intensity profiles with a mode-field diameter of 10 μm. The propagation loss derived from the imaginary part of the propagation constant was found to be less than 0.35 cm^{-1}.

Waveguide characterization was performed with a linearly polarized beam of a cw Yb fiber laser operating at 1064 nm. The beam was coupled by the microscope objective to a polarization-maintaining fiber coupler (Gooch and Housego). The 90% output of the coupler was butt-coupled to the WSA with a length of 3.37 mm and placed on a high-precision six-axes translation stage. A drop of glycerine was used between end of the WSA and the output of the coupler to reduce reflections off the edges. Light coming from the opposite end of the WSA was collimated by an aspheric lens onto a power meter. The 10% output of the coupler was used for input power control. Figure 2 shows two measured dependences of WSA transmittance on the input power. The first curve (shown by triangles) corresponds to the input polarization parallel to the [100] crystal axis, and the second curve (shown by circles) is for the polarization direction inclined by 45 grad relative the first one (in other words, along the [110] crystal axis). The WSA output mode profile was controlled by replacing the power meter with a Spiricon InGaAs beam profiler in the adjustment process of light coupling to the WSA. The output mode profile was close to a Gaussian shape with the radius ω=4.5 μm (1/e level of field) for all input powers. The mode-field diameter at the 90% output of the coupler was 6.2 μm. The experimental curves can be theoretically treated as
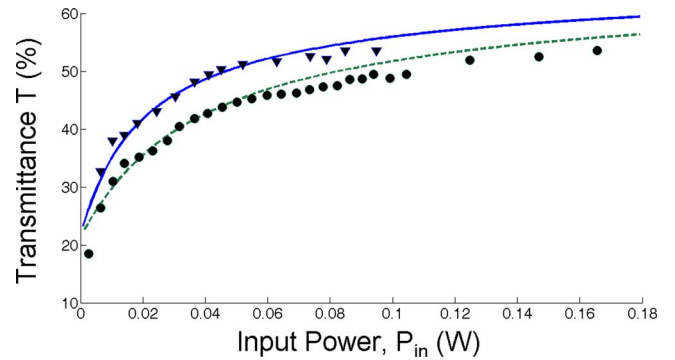

Fig. 2. (Color online) WSA transmittance versus input power at 1064 nm for polarizations along crystal axes: [100], triangles—experimental, solid curve—theoretical; [110], circles—experimental, dashed curve—theoretical.

$$T(P_{\mathrm{in}}) = \eta_{\mathrm{coup}} \times T_{\mathrm{WG}}(\eta_{\mathrm{coup}}P_{\mathrm{in}}, \alpha_{\mathrm{prop}}) \times (1 - R_F), \quad (1)$$

where η_{coup} is the coupling efficiency, T_{WG} is transmittance of the waveguide itself, α_{prop} is the nonsaturable loss that includes absorption of nonsaturable centers in the crystals and possible scattering added due to waveguide fabrication and coupling with cladding modes, and R_F=0.085 is the coefficient of reflection at a crystal facet (accounts for output coupling). The transmittance of waveguide T_{WG} was calculated on the basis of the well-known model of the Cr^{4+} centers, considering D$_{2d}$ as local symmetry. We used the following differential equation for evolution of Gaussian mode power $P(z)$ [10]:

$$\frac{\mathrm{d}P}{\mathrm{d}z} = -\frac{n}{3}\frac{\pi\omega^2 h\nu}{2\tau_1}\sum_{i=1}^{3}\ln\left(1 + \frac{2\tau_1\sigma_{0i}P(z)}{\pi\omega^2 h\nu}\right) - \alpha_{\mathrm{prop}}P(z).$$

$$(2)$$

Here n is the concentration of fourfold coordinated Cr^{4+} centers, τ_1 is their excited-state lifetime, and σ_{0i} are orientation-dependent absorption cross sections. For light polarized along the [100] crystal axis, σ_{01} = $\sigma_{0\pi}$ and σ_{02}=σ_{03}=$\sigma_{0\sigma}$, where $\sigma_{0\pi}$ is an absorption cross section for light polarized along the S$_4$ local axis of the Cr^{4+} center, and $\sigma_{0\sigma}$ is an absorption cross section for two other perpendicular directions. For light polarized along the [110] crystal axis, σ_{01}=σ_{02}=$(\sigma_{0\pi}$ +$\sigma_{0\sigma})/2$ and σ_{03}=$\sigma_{0\sigma}$. According to the results of the earlier modeling [10], no excited-state absorption was included in Eq. (1). We used the values of saturable absorption cross sections and excited-state lifetime $\sigma_{0\pi}$=4.5×10^{-18} cm^2, $\sigma_{0\sigma}$=1.5×10^{-19} cm^2, and τ_1 =4.0 μs for the YAG:Mg^{2+},Cr^{4+} crystal obtained in [10] in the numerical analysis of Eq. (2).

The theoretical dependence in Eq. (1) was fitted to the experimental curve by varying only the coupling efficiency and propagation losses. A good agreement between theory and experiment was found for α_{prop} =0.35 cm^{-1} and η_{coup}=92%. A small discrepancy at the high input power is apparently due to the decrease of the excited-state lifetime τ_1 caused by a waveguide core temperature rise. The lifetime has a strong temperature dependence [11], while in the
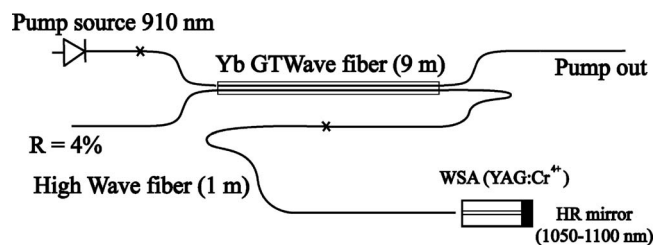
Fig. 3.   Laser experiment setup.

modeling the effects of crystal heating were neglected for simplicity. The results obtained indicate that the WSA possesses the absorption saturation parameters of the YAG:Cr^{4+} crystal, while the overall propagation losses are rather moderate.

The laser experimental configuration is shown in Fig. 3. A 9-m-long GTWave fiber [12] was used consisting of a Yb-doped fiber and a passive multimode fiber in a polymer protective coating with a refractive index lower than that for silica glass. In this design the pump power was delivered through the passive fiber. The concentration of Yb^{3+} ions in the active core was 5×10^{19} cm^{-3}; the mode field diameter was 5.7 μm. A 1-m-long undoped High Wave fiber with an 8.1 μm mode diameter was spliced to the active fiber core for better matching with the WSA, which has the larger mode diameter (9 μm). The WSA was butt-coupled to a cleaved end of the High Wave fiber. A drop of glycerin (with the refractive index matched to that of fused silica) between the fiber and the crystal was used to reduce parasitic reflection at surfaces of the fiber core. The adjacent crystal surface was anti-reflection coated. The opposite crystal surface was provided with an HR mirror coating for the 1050–1100 nm wavelength range. Thus, the laser cavity was formed by the HR mirror at the crystal end and one cleaved end of the active fiber core with a reflection coefficient of nearly 4%. A stable Q-switched oscillation at 1056 nm wavelength with the average output power of 23 mW and repetition rate of 20 kHz was demonstrated under cw pumping with 3 W power at 910 nm. Oscilloscope traces of Q-switch pulses were recorded using a New Focus InGaAs high-speed photodetector, Model 1611 (bandwidth of 0.03–1000 MHz) and a slow dc-coupled photodetector (Fig. 4). Further increase of the pump power led to an instability of the Q-switching regime caused by a chaotic self-Q-switch due to resonant absorption in Yb^{3+} ions. We believe that a spectral shift of the oscillation to a longer wavelength should suppress the self-Q-switch.

In conclusion, we have developed a saturable absorber for fiber lasers based on a femtosecond-inscribed waveguide in a YAG:Cr^{4+} crystal. Q-switched fiber laser operation using the new WSA was demonstrated.
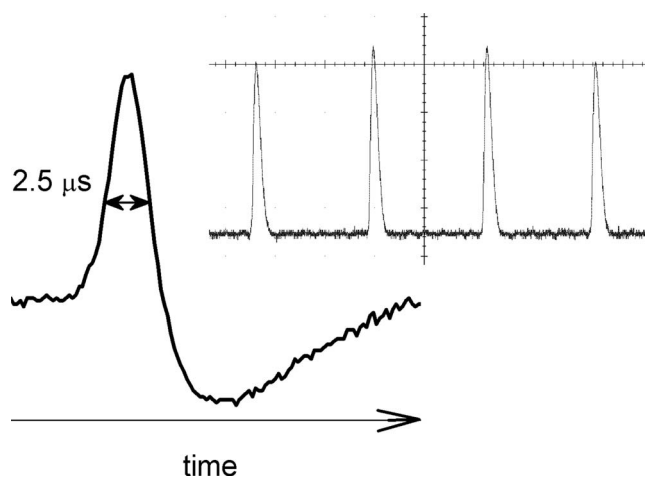

Fig. 4.   Traces of a Q-switch pulse recorded by fast (left) and slow photodetectors (right). The negative signal drop after the pulse is due to detector apparatus function.

References

1. V. V. Dvoyrin, V. M. Mashinsky, and E. M. Dianov, Opt. Lett. **32**, 451 (2007).
2. A. S. Kurkov, E. M. Sholokhov, and O. I. Medvedkov, Laser Phys. Lett. **6**, 135 (2009).
3. A. G. Okhrimchuk, A. V. Shestakov, I. Khrushchev, and J. Mitchell, Opt. Lett. **30**, 2248 (2005).
4. G. A. Torchia, A. Rodenas, A. Benayas, E. Cantelar, L. Roso, and D. Jaque, Appl. Phys. Lett. **92**, 111103 (2008).
5. J. Siebenmorgen, T. Calmano, K. Petermann, and G. Huber, in *Advanced Solid-State Photonics*, OSA Technical Digest Series (CD) (Optical Society of America, 2009), paper MB29.
6. A. G. Okhrimchuk, A. V. Shestakov, V. Mezentsev, and I. Bennion, XIII International Workshop OWTNM-2009, Jena, Germany, p. 71.
7. A. G. Okhrimchuk, A. V. Shestakov, V. Mezentsev, and I. Bennion, in *Conference on Lasers and Electro-Optics* (Optical Society of America, 2009), paper CJ7.4.
8. A. G. Okhrimchuk, V. K. Mezentsev, H. Schmitz, M. Dubov, and I. Bennion, Laser Phys. **19**, 1 (2009).
9. COMSOL Multiphysics, www.comsol.com.
10. A. G. Okhrimchuk and A. V. Shestakov, Phys. Rev. B **61**, 988 (2000).
11. A. G. Okhrimchuk and A. V. Shestakov, Opt. Mater. **3**, 1 (1994).
12. C. Codemard, K. Yla-Jarkko, J. Singleton, P. W. Turner, L. Godfrey, S.-U. Alam, J. Nilsson, J. Sahu, and A. B. Grudinin, Photon. Technol. Lett. **15**, 909 (2003).